Clim. Past, 4, 345–356, 2008
www.clim-past.net/4/345/2008/

Climate of the Past

The Southern Hemisphere at glacial terminations: insights from the Dome C ice core

R. Röthlisberger[1], M. Mudelsee[1,2], M. Bigler[3], M. de Angelis[4], H. Fischer[5,6], M. Hansson[7], F. Lambert[6], V. Masson-Delmotte[8], L. Sime[1], R. Udisti[9], and E. W. Wolff[1]

[1]British Antarctic Survey, Natural Environment Research Council, Cambridge, UK
[2]Climate Risk Analysis, Hannover, Germany
[3]Niels Bohr Institute, University of Copenhagen, Denmark
[4]Laboratoire de Glaciologie et Géophysique de l'Environnement, Grenoble, France
[5]Alfred Wegener Institut, Bremerhaven, Germany
[6]Climate and Environmental Physics, University of Bern, Switzerland
[7]Department of Physical Geography and Quaternary Geology, Stockholm University, Sweden
[8]Laboratoire des Sciences du Climat et de l'Environnement, Gif-sur-Yvette, France
[9]Department of Chemistry, University of Florence, Italy

Received: 21 May 2008 – Published in Clim. Past Discuss.: 19 June 2008
Revised: 12 September 2008 – Accepted: 22 October 2008 – Published: 9 December 2008

Abstract. The many different proxy records from the European Project for Ice Coring in Antarctica (EPICA) Dome C ice core allow for the first time a comparison of nine glacial terminations in great detail. Despite the fact that all terminations cover the transition from a glacial maximum into an interglacial, there are large differences between single terminations. For some terminations, Antarctic temperature increased only moderately, while for others, the amplitude of change at the termination was much larger. For the different terminations, the rate of change in temperature is more similar than the magnitude or duration of change. These temperature changes were accompanied by vast changes in dust and sea salt deposition all over Antarctica.

Here we investigate the phasing between a South American dust proxy (non-sea-salt calcium flux, nssCa^{2+}), a sea ice proxy (sea salt sodium flux, ssNa^{+}) and a proxy for Antarctic temperature (deuterium, δD). In particular, we look into whether a similar sequence of events applies to all terminations, despite their different characteristics. All proxies are derived from the EPICA Dome C ice core, resulting in a relative dating uncertainty between the proxies of less than 20 years.

At the start of the terminations, the temperature (δD) increase and dust (nssCa^{2+} flux) decrease start synchronously. The sea ice proxy (ssNa^{+} flux), however, only changes once the temperature has reached a particular threshold, approximately 5°C below present day temperatures (corresponding to a δD value of −420‰). This reflects to a large extent the limited sensitivity of the sea ice proxy during very cold periods with large sea ice extent. At terminations where this threshold is not reached (TVI, TVIII), ssNa^{+} flux shows no changes. Above this threshold, the sea ice proxy is closely coupled to the Antarctic temperature, and interglacial levels are reached at the same time for both ssNa^{+} and δD.

On the other hand, once another threshold at approximately 2°C below present day temperature is passed (corresponding to a δD value of −402‰), nssCa^{2+} flux has reached interglacial levels and does not change any more, despite further warming. This threshold behaviour most likely results from a combination of changes to the threshold friction velocity for dust entrainment and to the distribution of surface wind speeds in the dust source region.

1 Introduction

The climate of the late Quaternary has been marked by repeated changes between glacial and interglacial periods. The reasons for such changes are still not entirely understood, although it seems clear that orbital forcing and internal feedback mechanisms involving greenhouse gases play a vital role (Huybers, 2006; Köhler and Fischer, 2006 and references therein). There are various processes that are influenced by and that exert an influence on the evolution of

Correspondence to: R. Röthlisberger
(rro@bas.ac.uk)

Published by Copernicus Publications on behalf of the European Geosciences Union.

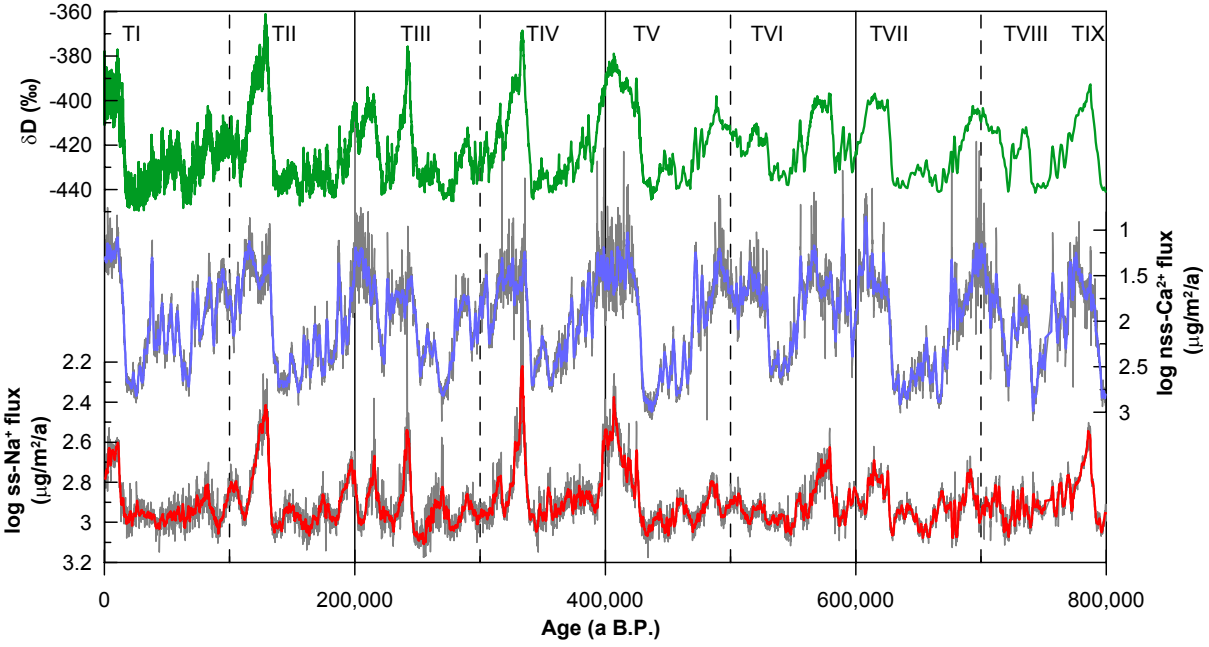

Fig. 1. Overview of entire data set. Shown are 0.55 m averages of δD (green) and 100 year averages of the logarithm of nssCa^{2+} and ssNa^{+} flux (grey) overlaid by a 11-point running average (blue, red). Y-axes of nssCa^{2+} flux and ssNa^{+} flux have been reversed in order to facilitate comparison with δD.

temperature and atmospheric CO_2. In high southern latitudes, the impact of sea ice extent and its connection to Southern Hemisphere winds and other factors that may contribute to ocean upwelling are of particular interest (Le Quere et al., 2007; Toggweiler et al., 2006).

The ice core from Dome C, Antarctica, that has been drilled in the framework of the European Project for Ice Coring in Antarctica (EPICA), provides a record of the last nine glacial – interglacial terminations in terms of changes in high latitude temperature (Jouzel et al., 2007), changes in greenhouse gases (Siegenthaler et al., 2005; Spahni et al., 2005) and various aerosols (Lambert et al., 2008; Wolff et al., 2006). Here we look into the pattern and phasing at terminations in different parameters, namely δD representing Antarctic temperature, nssCa^{2+} flux, a proxy for aspects of South American climate (Röthlisberger et al., 2002; Wolff et al., 2006), and ssNa^{+} flux, which is related to the sea ice extent around Antarctica (Wagenbach et al., 1998; Wolff et al., 2003). The aim is to identify robust pattern and phase-relationships at glacial terminations between Antarctic temperature, South American conditions and the sea ice based on the ice core record from Dome C.

2 Methods

2.1 Data

The ice core was drilled from 1996 to 2004 and has been analysed for stable water isotopes (δD, (Jouzel et al., 2007)) at 55 cm resolution. The analysis of the soluble impurities e.g. sodium (Na^{+}) and calcium (Ca^{2+}) has been done by seven European laboratories with different methods, and low-resolution data along most of the core, using a previous age-scale, have already been published (Wolff et al., 2006). In this study, we used the data obtained by continuous flow analysis (CFA), (Röthlisberger et al., 2000), which resulted in a high-resolution record (of the order of 1 cm, corresponding to less than a year in the Holocene, approximately 3 years at 410 ka BP during marine isotope stage (MIS) 11, and 20 years at 800 ka BP during MIS 20). In the top part (0 to 450 ka BP), these data were downsampled to 20 years resolution by using the median of the data in each 20-a interval in order to reduce the computing time. Below that, computing time was within reasonable limits for the high-resolution data, so that 1 cm data were used for further analysis. Fluxes, being representative of atmospheric concentrations at sites where dry deposition is assumed to dominate, were calculated using the accumulation rates derived from the EDC3 timescale (Parrenin et al., 2007) (Fig. 1). Compared to nssCa^{2+} and ssNa^{+} flux, the accumulation rate changed independently during terminations,

thus the uncertainty in reconstructing accumulation rate will translate into the $ssNa^+$ and $nssCa^{2+}$ fluxes. However, in view of flux changes of the order of a factor of 2 to 4 in $ssNa^+$ fluxes and 7 to 30 in $nssCa^{2+}$ fluxes over the nine glacial-interglacial terminations, the 30% uncertainty in accumulation rate is relatively small.

Both Ca^{2+} and Na^+ in the ice core originate from sea salt aerosol and terrestrial dust. However, Ca^{2+} is predominantly of terrestrial origin, while Na^+ derives mainly from sea salt. We calculated the non-sea-salt fraction of Ca^{2+} of terrestrial origin ($nssCa^{2+}$) and the sea-salt fraction of Na^+ ($ssNa^+$) as in Röthlisberger et al. (2002), using a Ca^{2+}/Na^+ weight ratio of 1.78 for terrestrial material (Rt), and 0.038 for sea water (Rm). The contribution from crustal material to total Na^+ depends on the composition of the dust source material, and higher ratios Rt of the terrestrial source material could be used (Bigler et al., 2006), resulting in lower $ssNa^+$ concentrations during glacial periods, but hardly any changes for interglacial periods. The effect of choosing different values for Rt on $nssCa^{2+}$ is negligible. For the aim of this study, the exact amplitude of glacial-interglacial changes in $ssNa^+$ does not affect the timing of the changes, and the results remain within error bars regardless of which values are used to calculate $ssNa^+$ and $nssCa^{2+}$.

All parameters were measured along the same core, i.e. the records are all on the same timescale (EDC3, Parrenin et al., 2007). The uncertainty in matching the three parameters is always much smaller than the resolution of δD. Therefore, the data offers excellent control of the relative timing between the proxies. However, the uncertainty of the absolute age is estimated 3 ka at 100 ka BP and approximately 6 ka for older sections of the ice core. In terms of event durations, the accuracy of the chronology is estimated to be 20% back to 410 ka BP and possibly 40% for older sections (Parrenin et al., 2007).

2.2 RAMPFIT

In order to estimate the exact timing of a glacial termination in an objective way, we used a regression approach (RAMPFIT, (Mudelsee, 2000)). RAMPFIT is a weighted least-squares method that fits a ramp to the data. It estimates the level of a parameter for glacial ($x2$) and interglacial ($x1$) conditions and a linear change between the change points $t1$ and $t2$ (Fig. 2). A measure of the uncertainty of these estimated change points is based on a set of 400 bootstrap simulations for each parameter and each termination (Mudelsee, 2000; Politis and Romano, 1994).

A simulated time series is generated by adding a sequence of successive residuals to the fitted ramp. The length of the sequence of residuals is defined by the persistence of the data (four times the persistence time), thus preserving the autoregressive properties of the original data in the simulated time series. The ramp fitting is then repeated on the simulated data, giving a set of simulated ramp parameters, $t1^*$, $x1^*$, $t2^*$ and $x2^*$. This procedure is repeated 400 times, and the standard deviation of these 400 $t1^*$ values is used as bootstrap standard error for $t1$ (see histograms in Fig. 2). The bootstrap standard errors for $x1$, $t2$ and $x2$ were calculated analogously.

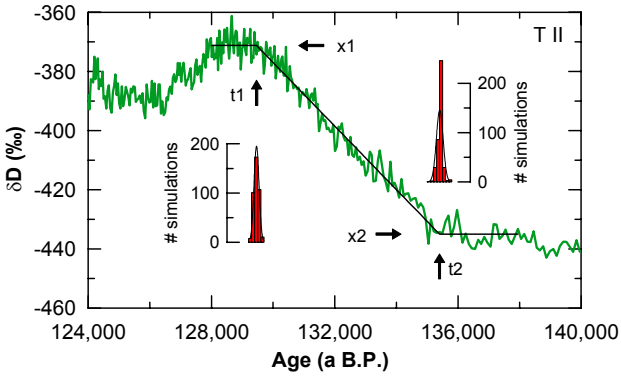

Fig. 2. Example of RAMPFIT results for δD at Termination II. The black line represents the ramp that best fits the data based on weighted least-squares regression. Arrows indicate the levels $x1$ and $x2$ and the change points $t1$ and $t2$. The histograms show the change points for 400 bootstrap simulations. The distribution of these simulated change points is used to derive an estimate of the uncertainty of the change points.

While the algorithm of RAMPFIT provides an objective estimate for the change points in a given data set, there are nevertheless some parameters that need to be chosen subjectively in the fitting procedure (e.g. the selection of the fit interval) that influence the result. For this study, we normally chose 2 ka beyond either end of the termination. In some instances, we chose shorter intervals in order to exclude sections of the data that had large deviations from a constant level and would thus distort the ramp. The parameters used for each termination are listed in the supplementary material (Table S1: http://www.clim-past.net/4/345/2008/cp-4-345-2008-supplement.pdf).

RAMPFIT minimizes the systematic deviations from constant glacial and interglacial levels and from the assumed linear change from glacial to interglacial conditions. However, a glacial termination does not necessarily conform to this simplified shape. For example, the interglacial levels need not be constant, or the termination may not progress linearly, but may change slope over time. This is illustrated in Fig. 3, where the Termination IV in $nssCa^{2+}$ flux is shown. Assuming a linear change over the entire termination results in change points that deviate from the change points that result from the assumed two-step termination. Alternatively, the glacial or interglacial levels are not constant, as for example the interglacial levels in δD in Termination III and IV, which reach high values early in the interglacial, but drop after a few thousand years (Fig. 4). This impacts the resulting levels and thus change points that RAMPFIT estimates. In other

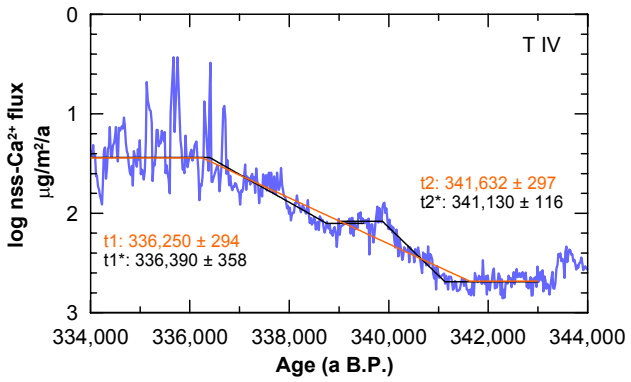

Fig. 3. Example of RAMPFIT results for nssCa^{2+} flux at Termination IV. The y-axis has been reversed. The orange line corresponds to a ramp fitted over the entire section; the black lines correspond to two separate ramps. The estimated change points are given for the single ramp ($t1$, $t2$) and for the corresponding two-step ramp ($t1$*, $t2$*).

words, the choice of the fit interval used for RAMPFIT had some influence on the resulting change point estimates.

While we are aware of the limitations of the ramp model, we still think it provides valuable insights into the phasing at glacial terminations. A model is supposed to bring out the major properties of a system rather than reflecting the full complexity of the data. Additional parameters in a model that would lead to a better fit between model and data do not necessarily improve the understanding of the system. In the case of quantifying phasing at glacial terminations as presented in this paper, we decided that a ramp, and in some cases a two-step ramp, provides a sufficiently complex description of the data, especially for the main purpose of defining change points.

2.3 Model experiments

Experiments using the HadAM3 model (Pope et al., 2000) were made in order to investigate the relationship between climate parameters in South America and Antarctica. In particular, we looked into the response of westerly winds to changes in sea surface temperatures (SST), and how the changes in winds relate to changes in Dome C temperature.

The atmospheric model HadAM3 has a regular latitude longitude grid with a lower horizontal resolution of $2.5° \times 3.75°$, and 19 hybrid coordinate levels in the vertical. The model climatology is similar to that observed. Additionally, where run in its coupled state, the model produces realistic simulations of coupled wind-dependent low-frequency variability e.g. El Nino Southern Oscillation and North Atlantic Oscillation events (Gordon et al., 2000; Collins et al., 2001), suggesting its suitability for investigating the behaviour of the westerlies.

In order to study the sensitivity of the westerly winds to changes in sea surface temperature, a series of experiments using different prescribed SST patterns were made (Fig. 7). The SST patterns were designed as follows: One set of experiments, labelled GLO in Fig. 7, was run with SST being reduced globally by 1°C to 4°C. A second set of experiments (EXT) was run with only extratropical (30° to pole) SST being reduced by 1°C to 4°C, with a linear reduction of the cooling towards 0°C at 20° and no cooling over the tropics. In another set of experiments (GRA), SST cooling increases linearly from the equator to the polar regions. And experiments with increasing extensions of sea ice (ICE) without changes to SST were made to separate the effect of SST from sea ice. Further details of the model experiment setup are given in Sime et al. (2008).

3 Results and discussion

The final ramps as calculated using RAMPFIT are shown in Fig. 4 and the estimated change points and error estimates are given in Table 1. A schematic of a termination is shown in Fig. 5. Across all terminations, δD and nssCa^{2+} flux start to change synchronously (within error estimate, indicated by arrow (a) in Fig. 5), while ssNa^{+} flux shows a delayed onset of the glacial termination by a few thousand years (arrow (b) in Fig. 5). On the other hand, the end of the termination is normally synchronous between ssNa^{+} flux and δD (arrow (d) in Fig. 5). Interglacial levels of nssCa^{2+} flux are either reached at the same time as δD and ssNa^{+} flux (Terminations I, V, VI, VII, VIII) or several thousand years earlier (Terminations II, III, IV, IX; arrow (c) in Fig. 5). In Terminations VI and VIII, the amplitude of the temperature change was relatively small. In these terminations, ssNa^{+} flux did not change significantly.

The δD in the ice core record is used primarily as a proxy for Antarctic temperature. However, especially at glacial terminations, other factors that have an influence on δD such as isotopic composition of seawater, moisture source region and local topography changes potentially changed quite significantly too. Therefore, the timing of the change in temperature compared to the changes in δD may be different. However, the change point estimates with RAMPFIT were also done on the reconstructed Dome C temperature T_{site} (not shown), which takes changes in moisture source region into account (Stenni et al., 2003). Estimates for the beginning of interglacial periods ($t1$) tend to be a few hundred years later in T_{site} than in δD, however, considering the uncertainty in the estimates, the change points were not significantly different from the change points estimated based on δD.

While the time difference between the start of the deglaciation in δD and the change point in ssNa^{+} flux tends to vary between 1 and 5 ka, the level of δD (-420 ± 5‰) at the beginning of the termination in ssNa^{+} flux ($t2$) seems to be nearly constant over all terminations (Table 2). Similarly,

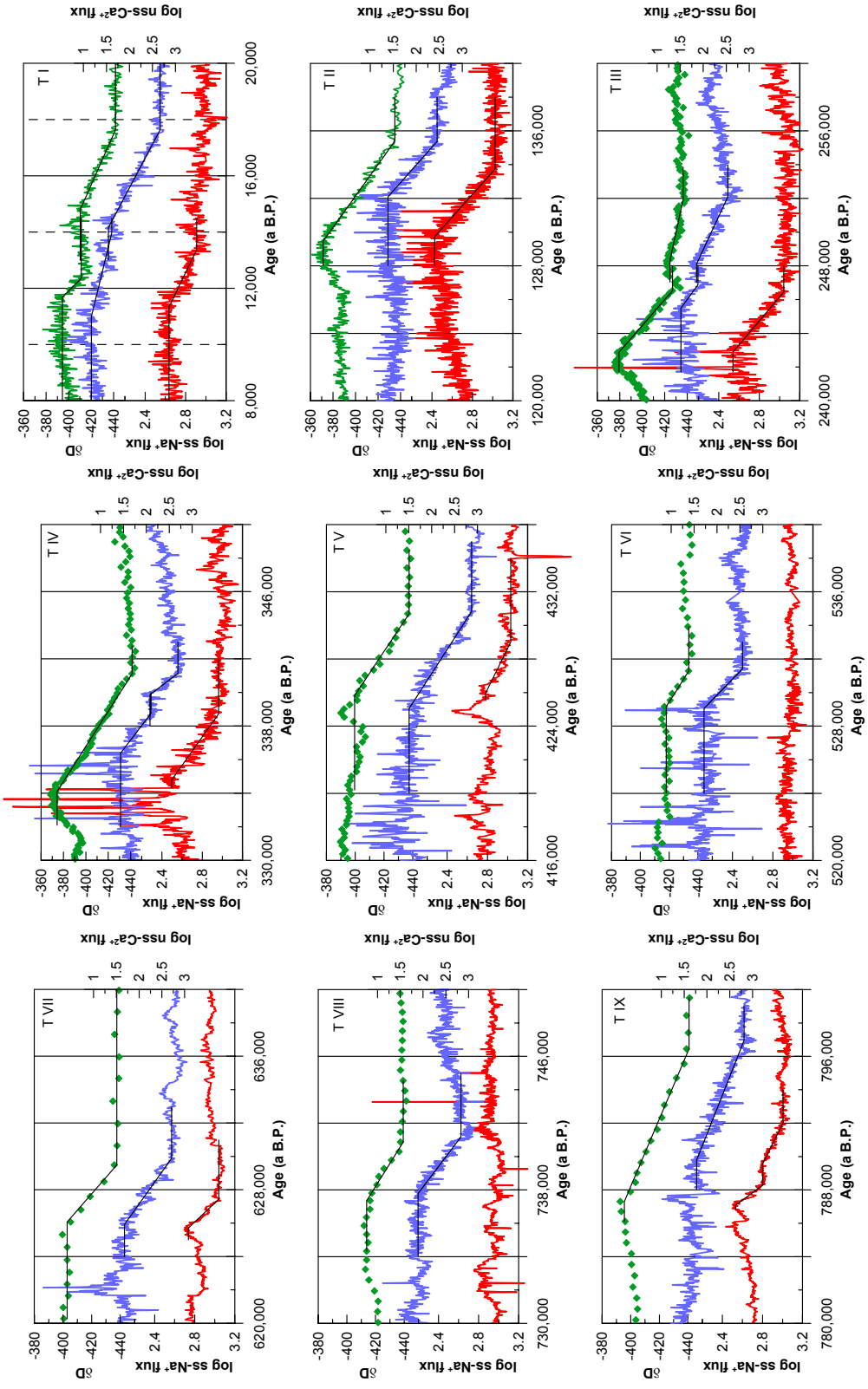

Fig. 4. Glacial terminations and ramps (black) estimated by RAMPFIT. δD in ‰(green), nssCa^{2+} (blue) and ssNa^{+} fluxes (red) in μg/m^2/a. Y-axes for ssNa^{+} and nssCa^{2+} have been reversed.

Table 1. The timing of glacial terminations in δD, log(nssCa^{2+} flux) and log(ssNa^{+} flux). $t1$ corresponds to the time when interglacial levels are reached, $t2$ to the time when the first deviation from glacial levels is observed. In some instances the analysis with RAMPFIT was done over two subsections in order to take account of a two-step shape of the termination. See methods for details regarding RAMPFIT. The uncertainty in $t1$ and $t2$ for δD is likely underestimated by RAMPFIT for Terminations VI, VII, VIII, IX due to the coarse temporal resolution of the data. For these terminations, the values in brackets are derived by RAMPFIT. The values in italic correspond to the average spacing of the data at that age, which is used as an estimate of the uncertainty.

Term.	δD				nssCa^{2+}				ssNa^{+}			
	$t1$	$\pm$	$t2$	$\pm$	$t1$	$\pm$	$t2$	$\pm$	$t1$	$\pm$	$t2$	$\pm$
I	11 686	235	12 350	252	10 990	620	13 970	548	11 330	186	13 370	239
	14 796	147	17 630	150	14 150	132	17 630	86				
II	129 459	82	135 402	110	132 091	190	135 371	110	129 731	192	133 731	103
III	242 867	111	246 528	148	245 491	354	246 871	339	242 891	455	246 451	202
	248 293	641	251 915	718	248 111	347	252 091	303				
IV	334 103	301	341 121	403	336 392	358	338 752	353	334 792	313	338 732	198
					339 872	114	341 132	116				
V	425 813	*471*	430 693	*617*	425 053	201	430 833	151	425 973	426	429 013	405
VI	529 157	(246) *340*	531 284	(233) *540*	529 055	234	531 405	203				
VII	626 073	(83) *720*	629 486	(58) *1320*	625 922	218	629 886	203	625715	158	627 438	129
VIII	737 354	(225) *580*	740 867	(214) *590*	737 784	184	741 171	192				
IX	787 298	(221) *640*	796 449	(106) *1040*	789 788	325	796 937	346	787 083	96	788 270	70
									789 590	128	792 007	115

Table 2. Levels of δD at the change points of glacial sea salt ($t2_{\text{ssNaflux}}$) and interglacial dust ($t1_{\text{nssCaflux}}$). Missing values in $t2_{\text{ssNaflux}}$ and values in parentheses in $t1_{\text{nssCaflux}}$ represent terminations where the thresholds for ssNa^{+} flux and nssCa^{2+} flux were not reached.

Termination	δD (‰) $t2_{\text{ssNaflux}}$	δD (‰) $t1_{\text{nssCaflux}}$
I	−412.6	−392
II	−416.2	−401.1
III	−426.8	−413.2
IV	−419	−400.4
V	−426.4	−392.8
VI	–	(−416.6)
VII	−419	−405.3
VIII	–	(−417.4)
IX	−420.2	−407.2
Average	−420	−402
Standard deviation	5.1	7.6
Standard error	1.9	2.9

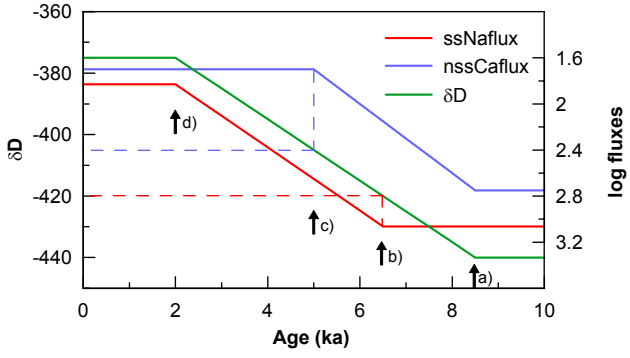

Fig. 5. Schematic of a glacial termination. Arrows indicate change points in nssCa^{2+} flux and ssNa^{+} flux (Y-axis for log fluxes reversed). Dashed lines indicate the threshold levels in δD.

the timing of the end of the termination in nssCa^{2+} flux ($t1$) and δD varies considerably (0 to 2.5 ka), but the level of δD (-402 ± 8‰) is more or less constant (Table 2). In other words, there are threshold levels in δD that correspond to the onset of changes in ssNa^{+} flux and to the end of

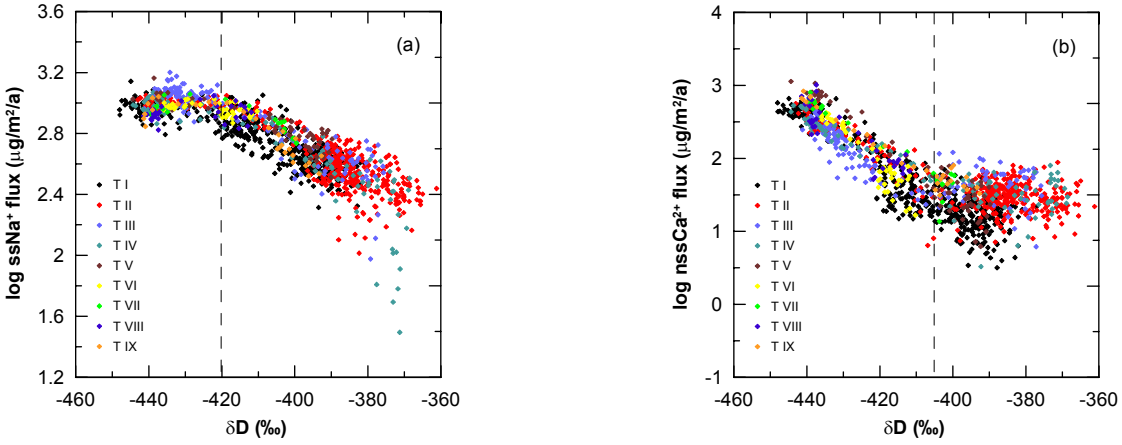

Fig. 6. Sea salt **(a)** and dust flux **(b)** versus δD over glacial terminations. The thresholds are indicated by a vertical dashed line. They are reflected in the different slopes in the relationship between sea salt (dust) and δD above and below the thresholds. The data from each termination are plotted in a different colour.

changes in nssCa^{2+} flux. These thresholds give rise to the apparent phase lags at the start or end of terminations. At glacial inceptions, the same threshold value seems to hold for ssNa^{+} flux (not shown). However, nssCa^{2+} flux tends to build up more gradually at glacial inceptions. Nevertheless, the threshold found for glacial terminations defines the level below which the millennial-scale variability in nssCa^{2+} flux correlates with δD.

These thresholds are illustrated in Fig. 6. While there seems to be a fairly close relationship between nssCa^{2+} flux and δD during glacial periods up to δD of approximately -402‰, the relationship vanishes beyond this point and nssCa^{2+} flux seems to be unrelated to δD. For ssNa^{+} flux, there is a good correlation with δD for values higher than approx. -420‰, however, below that, the ssNa^{+} flux seems to stay more or less constant.

3.1 Coupling of South America and Antarctica

The generally close coupling between South American dust flux and Antarctic climate during cold glacial conditions has been discussed recently based on the dust particle numbers in the Dome C ice core compared to δD (Lambert et al., 2008), and similar threshold levels below which the coupling manifests itself are derived. The factors that could influence the dust deposition in Antarctica are various parameters at the source (size of source area; conditions at the source, i.e. soil moisture, surface wind speed, vegetation, snow cover), atmospheric long-range transport (i.e. wind systems and wind speed) as well as the atmospheric lifetime of the dust particles. The implication of the threshold is that there is a point in the evolution of the climate system (represented by Antarctic temperature) beyond which one or more of these factors either ceases to change or ceases to influence dust.

Based on various transport models, changes in long-range transport (e.g. shorter transport times due to stronger winds) are unlikely to account for a large proportion of the observed changes (Krinner and Genthon, 2003; Lunt and Valdes, 2001), in line with evidence based on the size distribution of the dust particles (Lambert et al., 2008). Based on the comparison of the dust records from the two EPICA ice cores, Fischer et al. (2007) conclude that transport and lifetime effects have changed dust fluxes in Antarctica by less than a factor of 2, while Lambert et al. (2008) suggest that approximately a factor 5 of the glacial-interglacial change in dust flux might be explained by changes to the atmospheric lifetime while another factor of 5 is due to changes at the source. However, the change in atmospheric lifetime due to a reduced hydrological cycle is difficult to quantify. Results from a dust tracer model forced by a GCM showed only a marginal increase in lifetime, although with considerable uncertainty due to a poorly constrained scavenging ratio (Lunt and Valdes, 2002). The model produced a greatly increased Patagonian dust source during the LGM, mostly due to a decrease in soil moisture, with some contribution of decreased vegetation and increased land area during periods of low sea level.

Based on results from an atmospheric general circulation model (HadAM3), we looked into the relationship between changes in temperature at Dome C and various parameters of South American climate. The model provides a good representation of the present-day westerlies (Sime et al., 2008) and modern Antarctic climatology (Connolley and Bracegirdle, 2007). In order to study the sensitivity of the South American climate to changing conditions, several model experiments were run with the present-day setup but with imposed sea surface temperature (SST) anomalies (Sime et al., 2008).

A robust result from the Sime et al. study is the weakening of the westerly winds over southern high latitudes associated

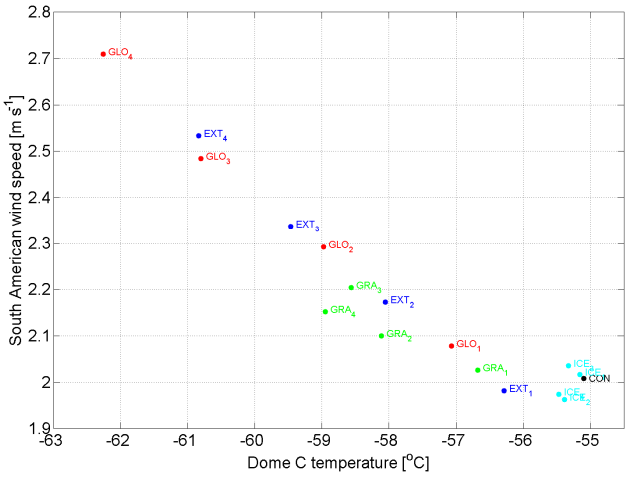

Fig. 7. Relationship between South American wind speed and temperature at Dome C for a set of experiments with the Hadley centre atmospheric general circulation model HadAM3. Each data point represents annual average wind speeds over South American landmasses south of 40° S against modelled temperature at Dome C for different model experiment. GLO experiments have uniform SST cooling from present-day conditions which range form 1 to 4°C as indicated by the subscript. EXT experiments have uniform SST cooling from present-day conditions over latitudes poleward of 30°, with a linear reduction towards 0°C cooling at 20° and no cooling over the tropics. GRA experiments have a zonally uniform SST cooling which linearly increases from the equator to the Polar Regions. ICE experiments have increasing extensions of sea-ice. Further experiment details are available in Sime et al.

with a warming at Dome C. This weakening appears to depend on a reduction in the meridional surface temperature gradient across the Southern Hemisphere; the gradient itself is generally dominated by changes in Antarctic temperature. The weakening simulated is liable to cause changes in dust transport. However, Lunt and Valdes (2001) note that changes of this type cannot be responsible for more than a small fraction of the dust changes seen in the Dome C record.

Over the South American dust entrainment region, the wind speed also decreases in response to Dome C warming. Figure 7 shows that for simple zonally uniform SST anomaly experiments, the mean annual wind speed over South America depends almost linearly on Dome C temperature. This is partly dependent on latitudinal shifts in the belt of the westerlies, but changes in the intensity and width of the wind band also play a significant role (Sime et al., 2008). Further experiments in Sime et al. (2008) indicate that the magnitude of the decrease is dependent on zonal variations in SST anomalies (not shown here). However, the general wind speed decrease is robust over the range of realistic experiments performed.

Dust entrainment is non-linearly related to surface wind speed, so that a modest decrease in surface wind speed at the most relevant latitudes could lead to a strong change in dust entrainment. This could therefore provide a link between the dust entrainment and the temperature at Dome C. The effect of changes in SST on dust entrainment may also be influenced by associated changes in precipitation. Increasing Southern Hemisphere SST leads to increased precipitation over Patagonia, therefore reducing the potential dust uplift due to raised soil moisture. Increased precipitation also promotes vegetation cover, as the major limiting factor for vegetation growth in Patagonia is precipitation (Markgraf et al., 2002), which further reduces dust uplift. Additionally, changes in South American topography due to ice cap disintegration at glacial terminations may have had an influence on wind pattern over the South American dust source.

From this analysis it is difficult to distinguish between the possible impacts of wind changes over dust source regions and of non-linear processes involved in dust entrainment. It is likely that the threshold velocity for dust entrainment was reduced during glacial periods due to less precipitation and therefore less vegetation cover. Additionally, the average wind speed was increased during glacial periods, and potentially also the gustiness (i.e. the likelihood of substantially higher than average wind speeds over short periods of time). Due to the non-linear relationship between dust entrainment and wind speed, especially near an entrainment threshold, even small increases in average wind speeds and gustiness could have a significant impact on dust entrainment. The combination of the changes in wind speed distribution and threshold velocity could qualitatively explain the observed threshold behaviour in the Dome C nssCa^{2+} flux record. The low dust flux levels during mild stages could thus reflect average wind speeds falling below the entrainment threshold, possibly in combination with reduced gustiness and higher threshold velocities due to increased soil moisture and vegetation cover. However, in order to make a quantitative assessment of the causes for the threshold found in the nssCa^{2+} flux record at Dome C, a model with a higher resolution that includes tracer uplift and transport is required.

3.2 Sea salt – sea ice relationship

In Antarctica, a large proportion of sea salt aerosol originates from sea ice surfaces rather than open water (Rankin et al., 2000; Wagenbach et al., 1998; Jourdain et al., 2008). Therefore, sea salt fluxes at Dome C have been used to infer past changes in sea ice extent in the Southern Ocean sector close to Dome C (Wolff et al., 2006; Wolff et al., 2003). As a first order approximation, one would expect to see a coupling between Antarctic temperature and sea ice extent. This should manifest in a general agreement in the δD and ssNa^{+} flux records from Dome C. While there indeed seems to be a strong correlation between δD and ssNa^{+} during mild stages ($r=-0.80$, significant at the 95% confidence level (Mudelsee, 2003), using 55 cm averages for ssNa^{+} flux and δD and

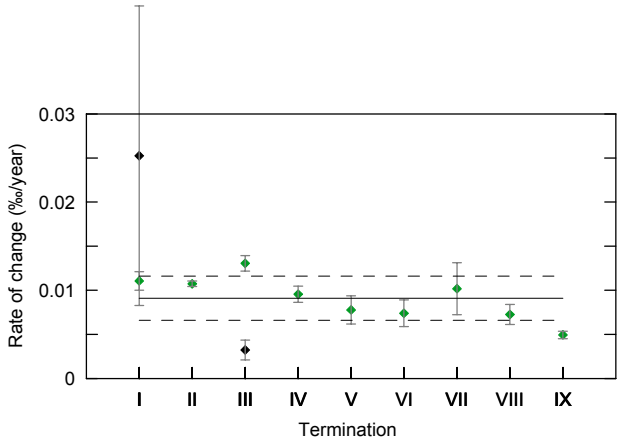

Fig. 8. Rate of change calculated based on termination ramps in δD. For T I and T III, two ramps were fitted to the data (see Fig. 4 and Table 1), and the rate of change has been calculated for each ramp separately. Error bars correspond to one standard error. The black diamond at T I corresponds to the short warming around 12 ka BP. It seems as if this warming was exceptionally fast, however, the uncertainty is large due to the short duration compared to the uncertainty in the determination of $t1$ and $t2$. The early part of Termination III seems to be exceptionally slow (black diamond) compared to the other terminations (see also Fig. 4). Also, Termination IX seems to progress slower than average. However, the uncertainty of the rate of change is most likely considerably underestimated. The horizontal lines represent the average rate of change of 0.0091±0.0025‰/year , calculated from all data except the two black data points.

all data with δD>-420‰), the relationship seems to break down during cold glacial conditions (r=−0.19, still significant at the 95% confidence level, for data with δD<-420‰). Obviously, during this time, one expects large sea ice extent around Antarctica, extending to over a thousand kilometres from the coast into the Southern Ocean (Gersonde et al., 2005). Sea salt aerosol produced at the distant margin of the sea ice cover will need to be transported over such long distances before reaching Dome C. However, it has been shown that the atmospheric sea salt aerosol concentration rapidly decreases with increasing transport distance, with only a small percentage of the original amount remaining after 500 km of transport (Minikin et al., 1994). Increasingly colder conditions will likely be accompanied by additional sea ice at the outer edge, at a distance of several hundred kilometres. But despite adding a considerable sea salt source area, the transport distance is so large that only a small fraction of this extra sea salt aerosol makes it to the East Antarctic plateau (Fischer et al., 2007). Although this requires confirmation, it appears likely that eventually, the effect of additional sea ice cannot be discriminated any more in the sea salt records. In other words, the sensitivity of sea salt flux at Dome C as a proxy for sea ice was decreased substantially during times of very large sea ice extent.

Table 3. Rate of change in δD over terminations.

Termination	Duration (years)	Change rate (‰/year)	±
Ia	664	−0.025	0.0170
Ib	2834	−0.011	0.0011
II	5943	−0.011	0.0003
IIIa	3661	−0.013	0.0009
IIIb	3622	−0.003	0.0011
IV	7018	−0.010	0.0009
V	4880	−0.008	0.0016
VI	2127	−0.007	0.0015
VII	3413	−0.010	0.0029
VIII	3513	−0.007	0.0011
IX	9151	−0.005	0.0004

In view of this, the delayed onset of changes in ssNa$^+$ flux with respect to the start of the warming at glacial terminations can be seen as the time when the sea ice proxy starts to respond to changes in sea ice again, i.e. when sea ice has retreated far enough so that further changes leave an imprint in the sea salt aerosol flux at Dome C. The end of the termination is synchronous in δD and ssNa$^+$, reflecting the expected relationship between Antarctic temperature and sea ice. A consequence of the reduced sensitivity of sea salt flux as a sea ice proxy during full glacial conditions is that we cannot infer the timing of sea ice changes in relation to changes in CO_2 at the start of a glacial termination based on the ice core record alone. Conclusions made in earlier papers (Röthlisberger et al., 2004; Wolff et al., 2006) require confirmation based on independent sea ice reconstructions.

3.3 Rate of change

The results from RAMPFIT can also be used to calculate the rate of change over each glacial termination. The glacial – interglacial amplitude is estimated as the difference between $x1$ and $x2$, while the duration of a termination and its uncertainty were calculated directly by RAMPFIT. The uncertainty in duration, as well as in $t1$ and $t2$ for δD (see Table 1), is likely underestimated by RAMPFIT for Terminations VI, VII, VIII, IX. This is caused by the coarse temporal resolution of the δD data. For these four terminations, the average spacing between data points is used as an estimate of the uncertainty of the change points and the duration, but this may still underestimate the true uncertainty.

As seen in Fig. 8, the rate of change in δD was rather similar for all terminations, of the order of 0.01‰/year, which is equivalent to approximately 2°C/ka. Only for the early part of Termination III and for Termination IX the temperature seemed to rise at a slower rate (see Table 3). This was also observed in the rate of change in nssCa^{2+} flux (Fig. S1: http://www.clim-past.net/4/345/2008/

cp-4-345-2008-supplement.pdf). The second warming step in Termination I, on the other hand, may have been exceptionally fast, as previously identified based on an independent analysis of the same data set (Masson-Delmotte et al., 2006). However, the uncertainty of this large rate of change is substantial, and the average rate of change observed during the other terminations lies well within the error bar. Generally, rates of change for $ssNa^{+}$ and $nssCa^{2+}$ flux over the corresponding intervals were also rather similar for all terminations. The first step in $nssCa^{2+}$ flux change at Termination IV was faster than average, however, it was followed by a period of rather constant $nssCa^{2+}$ flux (which was not seen in δD), before resuming the change into full interglacial conditions (see Fig. 4). Averaged over the entire Termination IV, the rate of change in $nssCa^{2+}$ flux was very similar to the one observed at other terminations.

This implies that regardless of the final amplitude of the glacial – interglacial temperature change, the climate system keeps changing at a steady pace. The duration of the termination is therefore shorter in the case where the interglacial temperatures were cool compared to the cases where rather warm interglacial temperatures were reached. This could be viewed as an external trigger (orbital forcing) timing the start of a glacial termination, but internal amplifiers and feedbacks (e.g. sea ice – albedo – temperature feedbacks or temperature – CO_2 feedbacks) governing the rate of change; the factors that determine at what point (in time or climate) the termination ends remain uncertain.

4 Conclusions

The analysis of the nine glacial terminations recorded in the Dome C ice core has provided insights into the phasing at glacial termination. Over all terminations, a consistent pattern emerged, involving threshold values beyond which a coupling between Antarctic temperature and Patagonian dust proxy ($nssCa^{2+}$ flux) on the one hand and the response of the sea ice proxy ($ssNa^{+}$ flux) on the other hand manifested itself.

Changes in South American dust emissions and Antarctic temperature are synchronous during cold glacial conditions but the dust response fades for conditions warmer than approximately 2°C below the present-day temperature at Dome C. The close link between dust and Antarctic temperature may be caused by the changes in wind pattern and precipitation over Patagonia that co-evolve with changes in temperature at Dome C.

Sea salt aerosol is closely linked to Antarctic temperature for interglacial conditions and conditions down to approximately 5°C cooler than present day. For these conditions, sea salt aerosol at Dome C can be used as a first-order proxy of sea ice in the Indian Ocean sector around Antarctica. For colder climate, the proxy is reaching some sort of saturation and fails to respond to potential further increases in sea ice extent. One result of this analysis is that we are no longer safe in suggesting that sea ice responded late in terminations and using this to apportion causes of CO_2 change; this conclusion was probably an artefact of the apparent threshold in response to sea ice change (Röthlisberger et al., 2004; Wolff et al., 2006).

The rate of change over glacial terminations as determined from the duration and the amplitude of the changes in δD seems to be rather similar over all glacial terminations. This suggests that once a glacial termination is triggered, the climate system progresses at its own pace. An exception with regard to this is a 3000 a period early on in Termination III where the rate of change seemed to be reduced significantly compared to the other terminations. It remains to be seen what caused this period to progress more slowly.

Acknowledgements. This work is contribution No. 211 to the European Project for Ice Coring in Antarctica (EPICA), a joint European Science Foundation/European Commission scientific programme, funded by the EU and by national contributions from Belgium, Denmark, France, Germany, Italy, The Netherlands, Norway, Sweden, Switzerland and the UK. The main logistic support at Dome C was provided by IPEV and PNRA.

Edited by: G. Lohmann

References

Bigler, M., Röthlisberger, R., Lambert, F., Stocker, T. F., and Wagenbach, D.: Aerosol deposited in East Antarctica over the last glacial cycle: Detailed apportionment of continental and sea-salt contributions, J. Geophys. Res., 111, D08205, doi:08210.01029/02005JD006469, 2006.

Collins, M., Tett, S. F. B., and Cooper, C.: The internal climate variability of HadCM3, a version of the Hadley Centre coupled model without flux adjustments, Clim. Dyn., 17, 61–81, 2001.

Connolley, W. M. and Bracegirdle, T. J.: An Antarctic assessment of IPCC AR4 coupled models, Geophys. Res. Lett., 34, L22505, doi:22510.21029/22007GL031648, 2007.

Fischer, H., Fundel, F., Ruth, U., Twarloh, B., Wegener, A., Udisti, R., Becagli, S., Castellano, E., Morganti, A., Severi, M., Wolff, E. W., Littot, G. C., Röthlisberger, R., Mulvaney, R., Hutterli, M. A., Kaufmann, P., Federer, U., Lambert, F., Bigler, M., Hansson, M., Jonsell, U., De Angelis, M., Boutron, C., Siggaard-Andersen, M.-L., Steffensen, J. P., Barbante, C., Gaspari, V., Gabrielli, P., and Wagenbach, D.: Reconstruction of millennial changes in dust emission, transport and regional sea ice coverage using the deep EPICA ice cores from the Atlantic and Indian Ocean sector of Antarctica, Earth Planet. Sci. Lett., 260, 340–354, 2007.

Gersonde, R., Crosta, X., Abelmann, A., and Armand, L.: Sea-surface temperature and sea ice distribution of the Southern Ocean at the EPILOG Last Glacial Maximum – a circum-Antarctic view based on siliceous microfossil records, Quat. Sci. Rev., 24, 869–896, 2005.

Gordon, C., Cooper, C., Senior, C. A., Banks, H., Gregory, J. M., Johns, T. C., Mitchell, J. F. B., and Wood, R. A.: The simulation of SST, sea ice extents and ocean heat transports in a version

of the Hadley Centre coupled model without flux adjustments, Clim. Dyn., 16, 147–168, 2000.

Huybers, P.: Early Pleistocene glacial cycles and the integrated summer insolation forcing, Science, 313, 508–511, 2006.

Jourdain, B., Preunkert, S., Cerri, O., Castebrunet, H., Udisti, R., and Legrand, M. R.: Year round record of size-segregated aerosol composition in central Antarctica (Concordia station): Implications for the degree of fractionation of sea-salt particles, J. Geophys. Res., 113, D14308, doi:10.1029/2007JD009584, 2008.

Jouzel, J., Masson-Delmotte, V., Cattani, O., Dreyfus, G., Falourd, S., Hoffmann, G., Minster, B., Nouet, J., Barnola, J. M., Chappellaz, J., Fischer, H., Gallet, J. C., Johnsen, S., Leuenberger, M., Loulergue, L., Luethi, D., Oerter, H., Parrenin, F., Raisbeck, G., Raynaud, D., Schilt, A., Schwander, J., Selmo, E., Souchez, R., Spahni, R., Stauffer, B., Steffensen, J. P., Stenni, B., Stocker, T. F., Tison, J. L., Werner, M., and Wolff, E. W.: Orbital and Millennial Antarctic Climate Variability over the Past 800 000 Years, Science, 317, 793–796, 2007.

Köhler, P. and Fischer, H.: Simulating low frequency changes in atmospheric CO_2 during the last 740 000 years, Clim. Past, 2, 57–78, 2006,
http://www.clim-past.net/2/57/2006/.

Krinner, G. and Genthon, C.: Tropospheric transport of continental tracers towards Antarctica under varying climatic conditions, Tellus, 55B, 54–70, 2003.

Lambert, F., Delmonte, B., Petit, J.-R., Bigler, M., Kaufmann, P., Hutterli, M. A., Stocker, T. F., Ruth, U., Steffensen, J. P., and Maggi, V.: Dust-climate couplings over the past 800 000 years from the EPICA Dome C ice core, Nature, 452, 616–619, 2008.

Le Quere, C., Rodenbeck, C., Buitenhuis, E. T., Conway, T. J., Langenfelds, R., Gomez, A., Labuschagne, C., Ramonet, M., Nakazawa, T., Metzl, N., Gillett, N., and Heimann, M.: Saturation of the Southern Ocean CO_2 Sink Due to Recent Climate Change, Science, 316, 1735–1738, 2007.

Lunt, D. J. and Valdes, P. J.: Dust transport to Dome C, Antarctica at the Last Glacial Maximum and present day, Geophys. Res. Lett., 28, 295–298, 2001.

Lunt, D. J. and Valdes, P. J.: Dust deposition and provenance at the Last Glacial Maximum and present day, Geophys. Res. Lett., 29, 2085, doi:2010.1029/2002GL015656, 2002.

Markgraf, V., Webb, R. S., Anderson, K. H., and Anderson, L.: Modern pollen/climate calibration for southern South America, Palaeogeography, Palaeoclimatology, Palaeoecology, 181, 375–397, 2002.

Masson-Delmotte, V., Dreyfus, G., Braconnot, P., Johnsen, S., Jouzel, J., Kageyama, M., Landais, A., Loutre, M.-F., Nouet, J., Parrenin, F., Raynaud, D., Stenni, B., and Tuenter, E.: Past temperature reconstructions from deep ice cores: relevance for future climate change, Clim. Past, 2, 145–165, 2006,
http://www.clim-past.net/2/145/2006/.

Minikin, A., Wagenbach, D., Graf, W., and Kipfstuhl, J.: Spatial and seasonal variations of the snow chemistry at the central Filchner-Ronne Ice Shelf, Antarctica, Ann. Glaciol., 20, 283–290, 1994.

Mudelsee, M.: Ramp function regression: a tool for quantifying climate transitions, Comput. Geosci., 26, 293–307, 2000.

Mudelsee, M.: Estimating Pearson's Correlation Coefficient With Bootstrap Confidence Interval From Serially Dependent Time Series, Math. Geol., 35, 651–665, 2003.

Parrenin, F., Barnola, J.-M., Beer, J., Blunier, T., Castellano, E., Chappellaz, J., Dreyfus, G., Fischer, H., Fujita, S., Jouzel, J., Kawamura, K., Lemieux-Dudon, B., Loulergue, L., Masson-Delmotte, V., Narcisi, B., Petit, J.-R., Raisbeck, G., Raynaud, D., Ruth, U., Schwander, J., Severi, M., Spahni, R., Steffensen, J. P., Svensson, A., Udisti, R., Waelbroeck, C., and Wolff, E.: The EDC3 chronology for the EPICA Dome C ice core, Clim. Past, 3, 485–497, 2007,
http://www.clim-past.net/3/485/2007/.

Politis, D. N. and Romano, J. P.: The stationary bootstrap, J. Am. Stat. Assoc., 89, 1303–1313, 1994.

Pope, V. D., Gallani, M. L., Rowntree, P. R., and Stratton, R. A.: The impact of new physical parametrizations in the Hadley Centre climate model: HadAM3, Clim. Dyn., 16, 123–146, 2000.

Rankin, A. M., Auld, V., and Wolff, E. W.: Frost flowers as a source of fractionated sea salt aerosol in the polar regions, Geophys. Res. Lett., 27, 3469–3472, 2000.

Röthlisberger, R., Bigler, M., Hutterli, M., Sommer, S., Stauffer, B., Junghans, H. G., and Wagenbach, D.: Technique for continuous high-resolution analysis of trace substances in firn and ice cores, Environ. Sci. Technol., 34, 338–342, 2000.

Röthlisberger, R., Mulvaney, R., Wolff, E. W., Hutterli, M. A., Bigler, M., Sommer, S., and Jouzel, J.: Dust and sea-salt variability in central East Antarctica (Dome C) over the last 45 kyrs and its implications for southern high-latitude climate, Geophys. Res. Lett., 29, 1963, doi:1910.1029/2002GL015186, 2002.

Röthlisberger, R., Bigler, M., Wolff, E. W., Joos, F., Monnin, E., and Hutterli, M. A.: Ice core evidence for the extent of past atmospheric CO_2 change due to iron fertilisation, Geophys. Res. Lett., 31, L16207, doi:16210.11029/12004GL020338, 2004.

Siegenthaler, U., Stocker, T. F., Monnin, E., Lüthi, D., Schwander, J., Stauffer, B., Raynaud, D., Barnola, J.-M., Fischer, H., Masson-Delmotte, V., and Jouzel, J.: Stable carbon cycle-climate relationship during the late pleistocene, Science, 310, 1313–1317, 2005.

Sime, L., Le Quere, C., Kohfeld, K., De Boer, A., Bopp, L., Wolff, E. W., and Connolley, W. M.: Influence of changes in boundary conditions on Southern ocean winds at the last glacial inception, in preparation, 2008.

Spahni, R., Chappellaz, J., Stocker, T. F., Loulergue, L., Hausammann, G., Kawamura, K., Flückiger, J., Schwander, J., Raynaud, D., Masson-Delmotte, V., and Jouzel, J.: Atmospheric methane and nitrous oxide of the late pleistocene from Antarctic ice cores, Science, 310, 1317–1321, 2005.

Stenni, B., Jouzel, J., Masson-Delmotte, V., Röthlisberger, R., Castellano, E., Cattani, O., Falourd, S., Johnsen, S. J., Longinelli, A., Sachs, J. P., Selmo, E., Souchez, R., Steffensen, J. P., and Udisti, R.: A late-glacial high resolution site and source temperature record derived from the EPICA Dome C isotope records (East Antarctica), Earth Planet. Sci. Lett., 217, 183–195, doi:110.1016/S0012-1821X(1003)00574-00570, 2003.

Toggweiler, J. R., Russell, J. L., and Carson, S. R.: Midlatitude westerlies, atmospheric CO_2, and climate change during the ice ages, Paleoceanography, 21, PA2005, doi:10.1029/2005PA001154, 2006.

Wagenbach, D., Ducroz, F., Mulvaney, R., Keck, L., Minikin, A., Legrand, M., Hall, J. S., and Wolff, E. W.: Sea-salt aerosol in coastal Antarctic regions, J. Geophys. Res., 103, 10 961–10 974, 1998.

Wolff, E. W., Rankin, A. M., and Röthlisberger, R.: An ice core indicator of Antarctic sea ice production?, Geophys. Res. Lett., 30, 2158, doi:2110.1029/2003GL018454, 2003.

Wolff, E. W., Fischer, H., Fundel, F., Ruth, U., Twarloh, B., Littot, G. C., Mulvaney, R., Röthlisberger, R., De Angelis, M., Boutron, C. F., Hansson, M., Jonsell, U., Hutterli, M. A., Lambert, F., Kaufmann, P., Stauffer, B., Stocker, T., Steffensen, J. P., Bigler, M., Siggaard-Andersen, M.-L., Udisti, R., Becagli, S., Castellano, E., Severi, M., Wagenbach, D., Barbante, C., Gabrielli, P., and Gaspari, V.: Southern ocean sea-ice extent, productivity and iron flux over the past eight glacial cycles, Nature, 440, 491–496, 2006.